Extension of Flocking Models to Environments with Obstacles and Degraded Communications

Alexandre Bonnefond, Olivier Simonin, Isabelle Guérin-Lassous

Extension of Flocking Models to Environments with Obstacles and Degraded Communications

Alexandre Bonnefond[1,2] and Olivier Simonin[1] and Isabelle Guérin-Lassous[2]

***Abstract*— In this paper, we study existing flocking models and propose extensions to improve their abilities to deal with environments having obstacles impacting the communication quality. Often depicted as robust systems, there is yet a lack of understanding how flocking models compare and how they are impacted by the communication quality when they exchange control data. We extend two standard models to improve their ability to stay connected while evolving in environments with different obstacles distributions. By taking into account the radio propagation, we model the obstacles impact on communications in a simulator that we use to optimize flocking parameters. The simulation results show the efficiency of the proposed models and how they adapt to different environmental constraints.**

I. INTRODUCTION

Since its formulation by Craig Reynolds [1] in 1987, the flocking theory has been of increasing interest. Based on three simple interactions between agents that are, the separation, the alignment and the cohesion (see Fig. 1), the author designed a decentralized system that can evolve in different types of environment. If this control strategy was originally designed for perception-based systems, the development of UAVs (Unmanned Aerial Vehicles) combined with improved communication abilities has made possible the adaptation of flocking to these types of vehicles. The agents are now able to exchange, via a high rate communication channel, crucial information such as their positions and velocities to their nearby "flockmates". As a consequence, most of the recent papers in the literature [2][3][4][5] consider communication-based flocking but without taking into account the real features of communications and how they are impacted by the presence of obstacles. The use of simple assumptions on communications appears to be one of the main issue when it comes to real experiments. The work of [6] gives a good idea of how realistic communications can affect an emergent behavior. However, the controller involved in this paper is quite simple and hence doesn't reflect how standard flocking models are affected. The objective of this article is to understand how the flocking models compare and how they are impacted by the quality of the communication, in terms of received power, when exchanging control data, this quality varying according to the distribution of obstacles. We also propose to extend two standard models (Olfati-Saber [2] and Vásárhelyi/Vicsek [4]) to improve their robustness in the presence of obstacles while designing decentralized flocking. We aim to maintain properties such as cohesion (avoiding fragmentation), non collision, alignment, and quality of communication. For this purpose, we use the stochastic framework of [7] to simulate and evaluate flocking models. We integrate in this simulator both realistic propagation models and various constrained environments including obstacles. Combined with an appropriate optimization process of the parameters, we show that the proposed flocking models remain robust even in highly constrained environments.

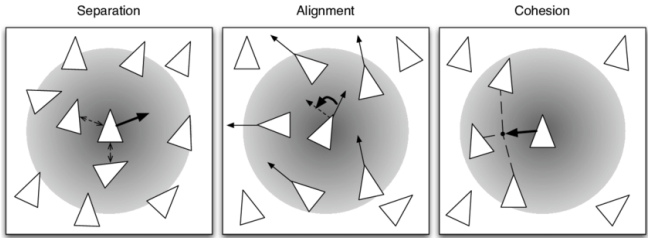

Fig. 1: Flocking : The 3 interactions defined by Reynolds (illustration from [8])

In Section II, we go through a non exhaustive list of existing flocking models with a focus on two specific models that we use in this article. In Section III, we describe the extension of the flocking models we propose. Then in Section IV, we present the models we consider for communications before redefining the notion of neighbourhood. We then compare these new models in Section V within different environments under varying constraints, specifically in terms of obstacles. We finally conclude with a discussion on how this framework could be extended.

II. EXISTING FLOCKING MODELS

Flocking models are usually applied to multi-agent systems in which a collective motion is aimed. Those models rely on three fundamental interactions introduced by Reynolds [1]:

- Collision Avoidance (or separation): avoid collision with nearby flockmates
- Velocity Matching (or alignment): attempt to match velocity (heading and amplitude) with nearby flockmates
- Flock Centering (or cohesion): attempt to stay close to nearby flockmates

where the flockmates are any agent in the system. Models are usually composed of N agents. Each agent i is referred to by its position $\mathbf{q}_i$ and velocity $\mathbf{v}_i$ (bold notation is used for vectors). It also has its set of neighbours with whom it

*This work is supported by the Inria-DGA DynaFlock project.

[1]INSA Lyon, CITI Lab., Inria Chroma team, 6 avenue des Arts, 69621 Villeurbanne, France firstname.lastname@inria.fr

[2]Lyon 1 University, LIP Lab., Inria Dante team, 46 allée d'Italie, 69364 Lyon Cedex 07, France firstname.lastname@ens-lyon.fr

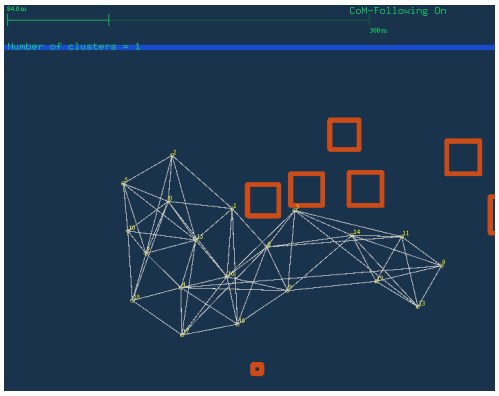

Fig. 2: Illustration of the Olfati-Saber model in the simulation framework, with 20 agents and communication links in white. The top green bar indicates the spatial scale.

interacts, denoted by:

$$N_i = \{j \in [\![1, .., N]\!]; j \neq i : |||\mathbf{q}_j - \mathbf{q}_i|| \leq r\} \quad (1)$$

where r is the interaction range. Most of the flocking models use these rules and definitions as a starting point, but when it comes to dynamics and control, different models are proposed. Among all the flocking models found in the literature, multiple strategies have emerged such as the leader-follower method [9][5], the potential field method [10], the behavior-based method [11], the virtual structure method [12] or the reinforcement learning method [13][14].

Because the flocking is now used to tackle problems with different goals, Reynolds' laws are embedded into complex multi-agent dynamics such as in the paper of Olfati-Saber [2] (denoted O-S hereafter). In his work, the author designs an appropriate mathematical framework to ensure the stability of his model. This aspect is important in the control theory and ensures a non erratic behavior which is highly desired for UAV-based applications for instance. O-S also introduces features like obstacle avoidance and a so-called "navigational feedback" giving a global direction to the agents, key parameter to avoid the fragmentation of the flock (*i.e.* the separation into multiple clusters). For these reasons, this model has been repeatedly used in the literature [15][14][16] with slight modifications and different purposes. The dynamics used in O-S is based on a double integrator with a velocity consensus protocol:

$$\begin{cases} \dot{\mathbf{q}}_i = \mathbf{v}_i \\ \dot{\mathbf{v}}_i = \mathbf{u}_i \end{cases}, \quad (2)$$

and the control input $\mathbf{u}_i$, applied to each agent i, relies on three terms:

$$\mathbf{u}_i = \mathbf{f}_i^g + \mathbf{f}_i^d + \mathbf{f}_i^\gamma, \quad (3)$$

where $\mathbf{f}_i^g$ is a gradient-based term merging both separation and cohesion, $\mathbf{f}_i^d$ is the velocity alignment term which acts as a damping force and $\mathbf{f}_i^\gamma$ is the so-called navigational feedback. This latter term acts as if there was a virtual leader whose parameters (location and velocity) are known by all the agents. As shown in Section III, we use part of the O-S's model as a first layer to build a new model that satisfies our objectives. Fig.2 shows the regular lattice agents achieve when applying O-S's model.

Another flocking mechanism that we use in this paper is the one introduced by Vicsek [17] in 1995, which considers that the particles or agents are "self-propelled". This characteristic, derived from ferromagnetic material observations, will be very important in our consideration as it leads to a *pure flocking* (*i.e.* purely decentralized). Based on this idea of self-propelling particles, Vásárhelyi et al. developed a framework [4] including a simulator which goes deep into the physical representation of the environment and the related constraints such as communication delays, inertia, refresh rate of sensors, locality of the communication, inaccuracy of on-board sensors and outer noises. The model is defined by an equation determining the acceleration $\mathbf{a}_i$ of each agent i (see [7]):

$$\mathbf{a}_i = \boldsymbol{\eta}_i + \frac{\mathbf{v}_i^d - \mathbf{v}_i - \mathbf{v}_i^s}{|\mathbf{v}_i^d - \mathbf{v}_i - \mathbf{v}_i^s|} \cdot \min\left\{ \frac{\mathbf{v}_i^d - \mathbf{v}_i - \mathbf{v}_i^s}{\tau_{CTRL}}, a_{max} \right\}, \quad (4)$$

where $\boldsymbol{\eta}_i$ models the outer noise (like the wind effect), $\mathbf{v}_i^s$ represents the inner noise on the velocity measurements (due to GPS approximations), τ_{CTRL} is the relaxation time of the velocity controller, a_{max} is the limit in acceleration and $\mathbf{v}_i^d$ is the desired velocity:

$$\mathbf{v}_i^d = \frac{\tilde{\mathbf{v}}_i^d}{|\tilde{\mathbf{v}}_i^d|} min\{|\tilde{\mathbf{v}}_i^d|, v^{max}\}, \quad (5)$$

where v^{max} is the maximal allowed speed of each agent and $\tilde{\mathbf{v}}_i^d$ is defined as:

$$\tilde{\mathbf{v}}_i^d = \frac{\mathbf{v}_i}{|\mathbf{v}_i|} v^{flock} + \mathbf{v}_i^{rep} + \mathbf{v}_i^{frict} + \sum_s \mathbf{v}_{is}^{wall} + \sum_s \mathbf{v}_{is}^{obstacle} \quad (6)$$

where $\mathbf{v}_i$ is the real velocity of the ith agent, v^{flock} is the preferred speed of the agents, $\mathbf{v}_i^{rep}$ is the repulsion term based on the half spring model, $\mathbf{v}_i^{frict}$ is the alignment term that synchronizes motion within the flock, $\mathbf{v}_{is}^{wall}$ and $\mathbf{v}_{is}^{obstacle}$ are the terms used for obstacles and walls avoidance. The combination of this control law as well as the integration of real outdoor experiment constraints makes this framework very attractive. This is why we use it in this paper to propose extended versions.

Although those different models reach good performances (like, for instance, stability, robustness, smooth behaviour) in simulation, they have issues when scaling up to real outdoor experiments. Indeed, as pointed out in [4], in practice, multiple communication outages happened and it is a major drawback when working with UAVs.

III. Flocking models extension

In order to avoid the pitfall experienced by the models presented in Section II when used in a realistic environment, we propose new flocking models. Those models exploit the fundamental interactions of the two models described previously and include additional features expected to be robust to degraded communications due to the presence of obstacles.

A. VAT Model: Vásárhelyi + Attraction

Backed by a robust behaviour, the velocity controller defined by Vásárhelyi (see Eq. 6) was originally designed without any attraction term. We observed that, within environments containing many obstacles, the repetitive obstacles avoidance maneuvers combined with degraded communications eventually lead to fragmentation. We hence decided to introduce an attraction term based on the half-spring model in order to enhance the cohesion whenever it is possible:

$$\mathbf{v}_{ij}^{att} = \begin{cases} p^{att}(r_0^{att} - q_{ij})\dfrac{\mathbf{q}_i - \mathbf{q}_j}{q_{ij}}, & \text{if } q_{ij} > r_0^{att} \\ 0, & \text{otherwise} \end{cases} \quad (7)$$

where p^{att} is a linear gain, $q_{ij} = |\mathbf{q}_i - \mathbf{q}_j|$ is the distance between agents i and j and r_0^{att} is the attraction range under which agents stop attracting each other so as to prevent additional collisions. Also we have $\mathbf{v}_i^{att} = \sum_j \mathbf{v}_{ij}^{att}$. Adding this term to the input control must be done carefully regarding the repulsion term in order to not have oscillations. Hence, we set r_0^{att} large enough for the agents to have a slack distance between attraction and repulsion. Our first proposition is hence a velocity-based model denoted VAT:

$$\tilde{\mathbf{v}}_i^d = \frac{\mathbf{v}_i}{|\mathbf{v}_i|} v^{flock} + \mathbf{v}_i^{rep} + \mathbf{v}_i^{att} + \mathbf{v}_i^{fric} + \sum_s \mathbf{v}_{is}^{wall,obst} \quad (8)$$

The obstacle and wall interactions are concatenated in the last term for convenience and Eq. 5 remains valid. This resulting desired velocity encompasses 12 parameters, acting on different terms of the law and producing different behaviours. We will see in Section V-B how those parameters are optimized to reach an optimal behaviour (see the attached video).

B. VOS Model: Vásárhelyi + Olfati-Saber

The second model we extend, denoted VOS, is based on a combination of O-S's model, exploiting the stability of the behaviour derived from using its control input (3), and some features of Vásárhelyi's model used to add self-propelling and obstacle avoidance abilities. To this end, we come up with a nested control structure merging both controllers:

$$\begin{cases} \mathbf{u}_i = \alpha \mathbf{f}_i^g + \beta \mathbf{f}_i^d & \text{(9a)} \\ \tilde{\mathbf{v}}_i^d = \dfrac{\mathbf{v}_i}{|\mathbf{v}_i|} v^{flock} + \sum_s \mathbf{v}_{is}^{wall,obst} + \int_{T_s} \mathbf{u}_i \, dt & \text{(9b)} \end{cases}$$

where α and β are some linear coefficients which compensate the delay introduced by the integration and $T_s = 1/f_s$ with $f_s = 100Hz$ the working frequency of the controller. The other terms have been defined in Section II. The objective here is to avoid the fragmentation by adding the self-propelling term ($v^{flock}.\mathbf{v}_i/|\mathbf{v}_i|$). We recall that in its original paper [2], O-S introduces a *navigational feedback* term to deal with the fragmentation ($\mathbf{f}_i^\gamma$ in Eq. 3). It is something we want to avoid here as it goes against our will of developing a fully decentralized system performing pure flocking. Even if we had kept the $\mathbf{f}_i^\gamma$ term, the stability of O-S's model would not be guaranteed because it relies on free-flocking [2], *i.e.* flocking in environments without obstacles. However we will see in Section V-C that VOS presents a good stability even with many obstacles.

As for the VAT model, the 10 parameters of the VOS model will be optimized before evaluation (see Sec. V-B).

IV. Communication and Neighbourhood in Presence of Obstacles

As mentioned earlier, most of the flocking simulations consider ideal communications and do not take into account the impact of the environment on the communication quality which usually results in issues when scaling up to real experiments. A majority of the simulations uses a distance threshold under which the communication is possible and above which it is not (parameter r of Eq.1) and the communication is either perfect [2][15], or more realistic (with added random delays and packet losses) [4][7]. In [3], the authors use the BER (Bit Error Rate) combined with the SNR (Signal to Noise Ratio) to characterize the communication quality and integrate it into a performance index expressing a trade-off between inter-agent distance and quality of the communication. In [18], the authors come up with an hybrid system combining a prediction step and a learning step of the path loss field. They use the SPLAT![1] tool to predict how the path loss field is affected by the topology of an area. Although this method gives realistic insights for the RF measurements, it does not tell how the multi-agent system is impacted by these fluctuations. On this subject, in [6], the authors explain how an emergent behavior, such as flocking, is impacted when we use a relatively accurate propagation model and tune the inherent losses due to shadowing effects, SNR, jamming and so on. However, these studies consider only simplistic flocking models, far from realistic fleet of UAVs.

We propose to use a communication model based on the path loss estimation, including the presence of obstacles. This allows us to redefine the neighbourhood definition and consequently to better estimate with whom each agent interacts.

In the following, we introduce a prediction step using the log distance path loss model (denoted LDPL) for both free space propagation but also inside obstacles and we see how heterogeneous environments affect the quality of the communications and consequently the flocking strategy.

A. Log Distance Path Loss model with environment losses

Instead of using distance-based communication model, we aim at modelling how radio waves dynamically evolve with the environment and affect the neighbourhood. To do so, we consider the LDPL model that predicts the path loss a signal encounters within different types of environments [19]. It is formulated as follows:

$$PL = P_{Tx_{dBm}} - P_{Rx_{dBm}}, \quad (10)$$

$$PL = \begin{cases} PL_0 + 10\gamma log_{10}\dfrac{d}{d_0} + X_g, & \text{if } d \geq d_0 \\ PL_0, & \text{otherwise} \end{cases} \quad (11)$$

[1]Information about SPLAT!: https://www.qsl.net/kd2bd/splat.html

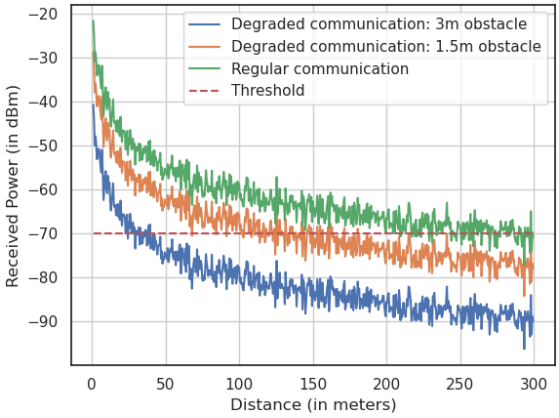

Fig. 3: Evolution of the received power as a function of inter-agent distance. The green line represents a path without obstacle, the orange line has a 1.5 meters long obstacle on its path and the blue one has a 3m long obstacle on its path

where, PL is the path loss measured in decibels (dB), $P_{Tx_{dBm}}$ is the transmitted power in dBm at the emitter, $P_{Rx_{dBm}}$ is the received power in dBm at the receiver, PL_0 is the path loss at the reference distance d_0 calculated using the Friis free-space path loss model, d is the distance between the emitter and the receiver, γ is the path loss exponent that depends on the environment (we use $\gamma = 2$ in free space) and X_g reflects the variations of the path loss caused by shadowing effects and/or multiple paths. This latter is a zero mean Gaussian random variable with a standard deviation of $\sigma = 2dB$. For the sake of clarity, we will refer to this communication model as **regular**. The green curve in Figure 3 represents the evolution of $P_{Rx_{dBm}}$ on a path where there is no obstacle and $P_{Tx_{dBm}} = 20dBm$. We can see that it takes approximately 300 meters to reach the power threshold $P_{min} = -70dBm$ which is often considered as the minimum level required to enable a reliable communication between agents in Wi-Fi for instance.

In the previous formula, the environment is modeled via, among others, the parameter γ and X_g. In order to better take into account the impact of the different obstacles on the communication quality, we add a dissipation model inside the obstacles leading to high loss of the signal strength when the signal goes through an obstacle. The resulting path loss is expressed as follows:

$$PL = \begin{cases} PL_0 + 10\gamma log_{10}(\frac{d - d_{obst}}{d_0}) & \text{if } d - d_{obst} \geq d_0 \\ + X_g + PL_{obst}(d_{obst}), & \\ PL_0 + PL_{obst}(d_{obst}), & \text{otherwise} \end{cases} \quad (12)$$

where, d_{obst} is the length of the path inside the obstacle and PL_{obst} is the path loss in dB due to obstacle attenuation. By using a simplified model of the path loss, this latter is defined as:

$$PL_{obst}(d_{obst}) = 10\gamma_{obst} log_{10}(d_{obst}) + K \quad (13)$$

where γ_{obst} is the path loss exponent for the obstacle and K is a constant. We assume that $d_{obst} \geq 1m$. This communication model will be called **degraded**. The orange and the blue curves in Figure 3 represent the evolution of $P_{Rx_{dBm}}$ on a path where respectively $d_{obst} = 1.5m$ and $d_{obst} = 3m$. In this configuration we have $\gamma_{obst} = 4$, $P_{Tx_{dBm}} = 20dBm$ and $K = 0$. We can see that this model has a strong impact on the communication's quality as it takes less than 30 meters to first lose the communication among agents with a 3 meters obstacle between them.

B. Neighbour Filtering

Thanks to Eq. 12, we are now able to redefine the neighbourhood N_i seen by agent i:

$$N_i = \{j \in [\![1, .., N]\!]; j \neq i : PL_{ij} \leq P_{threshold}\} \quad (14)$$

where PL_{ij} is the path loss (Eq. 12) measured from agents j to i and $P_{threshold}$ ($\neq P_{min}$) is the power threshold above which the communication is no longer possible. Also we introduce another threshold N_{max}, adjustable, which acts on the cardinality of N_i:

$$N_i = \begin{cases} N_i, & \text{if } |N_i| \leq N_{max} \\ N_i^{filtered}, & \text{otherwise} \end{cases} \quad (15)$$

where $N_i^{filtered}$ corresponds to a subset of N_i where the worst neighbors in terms of path loss are recursively removed until $|N_i| = N_{max}$. This feature is very important as it limits the computational costs of each agent while focusing the interactions on the most reliable flockmates. To add more realism, this neighbourhood is updated at the same frequency as the GPS since position information are needed to compute inter-distances. With this new definition of the neighbourhood, based on a more realistic communication model, we can study the evolution of a flock in highly constrained environments with multiple obstacles.

V. Comparison of models

A. Simulation framework

The simulator we use is an extension of the tool[2] developped by Viragh et al. [7], illustrated in Fig. 4. It is a multi-agent based simulator which introduces random variables for modelling noises on different variables, adding a complexity for both the resolution of the stochastic differential equations (SDE), using *Euler-Marayuma* method, but also the parameter optimization (see Section V-B). We decided to use this simulator instead of off the shelf simulators such as ARGoS or GAZEBO for two main reasons. The first one is that the original Vásárhelyi's model was already implemented in this simulator and hence would give us a fair comparison with our models. The second one, and probably the most important, is that we mostly use this simulator on servers to perform parameters optimization which requires hundreds of runs and this tool is well designed for that. The visualisation is only used to check the behavior of the agents for a given set of parameters.

[2]Access to the original project here: https://github.com/csviragh/robotsim

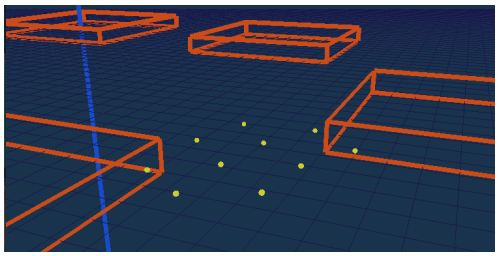

(a) 3D View of a "City" environment

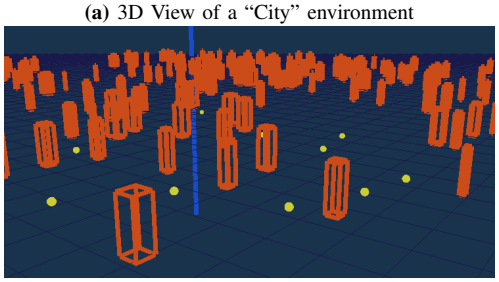

(b) 3D View of a "Forest" environment

Fig. 4: Simulator views

The hyper-parameters of an experiment such as its duration T or its calculation step for the Euler method are adjustable as well as the obstacle distribution defined by, among others, its density D which we measure as follows:

$$D = 100 \times \frac{\sum_s A_s}{A_{arena}}, \tag{16}$$

where A_s is the area of the sth obstacle and A_{arena} is the area of the arena. Figure 4(b) shows a 3D view of a so-called "Forest" environment as it has many small obstacles.

Several features have been added to this simulator to comply with our needs like the clusters detection using *Depth First Search* algorithm (DFS) over the graph of connected agents, the ability to switch on the fly the flocking model or the communication model (regular/degraded). See the attached video illustrating models simulation.

B. Parameter optimization

As we mentioned in Section III, the models we propose and study have several parameters that must be optimized to reach their best possible flocking behaviour. We took some inspiration from [4] to define different metrics so as to rate a flocking model:

- **Velocity**: $\Psi_{vel} = \frac{1}{T}\frac{1}{N}\int_0^T \sum_{i=1}^N |\mathbf{v}_i(t)|dt$, which characterizes the average velocity of the flock.
- **Collision** (between agents): $\Psi_{col} = \frac{1}{T}\frac{1}{N(N-1)}\int_0^N \sum_{i=1}^{N}\sum_{j\neq i}\Theta(q_{ij}(t) - r^{coll})dt$, evaluates the ratio of collision, with Θ the Heaviside step function and r^{coll} the minimum allowed distance between two agents.
- **Connected**: $\Psi_{clust} = \frac{1}{T}\int_0^T |\overline{O(t)}|dt$, $\underline{O(t)} = \{i \in [\![1, .., N]\!] : |N_i| = 0\}$, $\overline{O(t)}$ is the set of connected agents at t, ie. the complement of isolated agents $O(t)$.

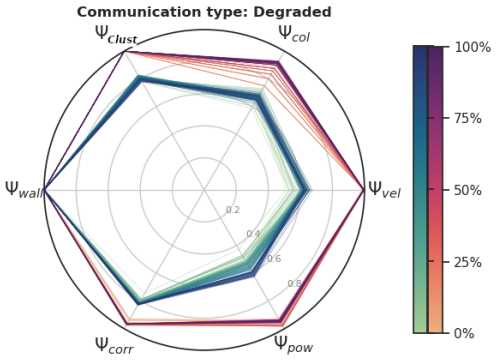

Fig. 5: Evolution of the metrics during optimization using degraded communication in the genetic env. (VAT in red, VOS in blue)

- **Wall** (collision): $\Psi_{wall} = \frac{\int_0^T \sum_{i=1}^N \Theta(\tilde{q}_{is}(t))\tilde{q}_{is}(t)dt}{\int_0^T \sum_{i=1}^N \Theta(\tilde{q}_{is}(t)dt}$, where $\tilde{q}_{is}$ takes positive values outside the arena and inside an obstacle, negative ones otherwise. Ψ_{wall} characterizes the average distance spent inside the obstacles.
- **Cluster Correlation**: $\Psi_{corr} = \frac{1}{T}\frac{1}{N}\int_0^T \sum_{i=1}^N \frac{1}{|N_i|-1}\sum_{j\in N_i}\frac{\mathbf{v}_i\cdot\mathbf{v}_j}{|\mathbf{v}_i||\mathbf{v}_j|}dt$, which gives a measure on the average alignment per cluster.
- **Cluster Received Power**: $\Psi_{pow} = \frac{1}{T}\frac{1}{N}\int_0^T \sum_{i=1}^N \frac{1}{|N_i|-1}\sum_{j\in N_i} P_{Rx_{ij}}(t)dt$, which gives a measure on the average received power per cluster.

Based on this, the following conditions are required to obtain an optimal flocking behaviour: $\Psi_{vel} \to v^{flock}$, $\Psi_{col} \to 0$, $\Psi_{clust} \to 1$, $\Psi_{wall} \to 0$, $\Psi_{corr} \to 1$, $\Psi_{pow} \geq P_{min}$. Those metrics are then passed into non-linear functions to map them between 0 and 1 (the sigmoid function for example), 0 being the worst case and 1 the best, to fit into a multi-objective optimization framework.

In this paper, we used *NSGA-III* [20][21] which is a fast non-dominated sorting genetic algorithm designed for multi-objective problems. This algorithm is however not suited for stochastic optimization but we modified it by evaluating the same solution several times and using the computed variances of the metrics as a constraint of the optimization. This leads to more robust solutions, less impacted by the randomness of an experiment.

Our strategy is to optimize both VAT and VOS models on a "generic environment", *i.e.* with an average density of obstacles, and with the *degraded* communication model. The number of agents used for the optimization step and the simulations whose results are given in Section V-C is the same: $N = 10$. Then we use those optimized versions on specific obstacle distributions to compare their performances. The generic environment has $N_{obst} = 90$ obstacles uniformly distributed on a 1250 m^2 arena. Each obstacle is represented by a square whose edge length L follows a normal (Gaussian) distribution $L \sim \mathcal{N}(\mu, \sigma)$, with mean $\mu = 24$m and a standard deviation $\sigma = 12$m. The average density $D = 3.3\%$. The optimization process is represented in Fig. 5 which

TABLE I: VAT and VOS optimized parameters in GENERIC env.

	Vel	Col	Clust	Wall	Corr	Pow
VAT	0.999	0.99	0.94	1	0.86	0.202
VOS	0.612	0.88	0.92	1	0.784	0.26

TABLE II: VA performances from [4]

	Vel	Col	Clust	Wall	Corr	Pow
VA	0.938	0.945	1	0.997	0.916	N/A

tracks the evolution of the average of the metrics of the Pareto set at each generation for both models (VOS in blue and VAT in red). The color-bar gives an index on how advanced we are in the optimization, based on a maximum number of generations. Although VOS seems to be outperformed by VAT, it is only because its Pareto front is bigger with broader elements than VAT one. Table I gathers the average metric values after 100 evaluations in the *generic* environment with *degraded* communication using the "best" solutions derived from the optimization for both models. One can observe that both models have close performances except for the *velocity* metric which is lower in VOS model. These solutions are carefully compared in the following subsection.

C. Simulation results

We aim here at comparing the VAT and VOS models inside different environments and using the different communication models we proposed (regular and degraded). The following comparison will be based on two different environments (see Fig. 4):

1) **Forest**: $N_{obst} = 500$; $L \sim \mathcal{N}(4,\, 2)$; $D = 0.7\%$.
2) **City**: $N_{obst} = 15$; $L \sim \mathcal{N}(200,\, 20)$; $D = 36.5\%$.

We will also make a comparison to Vásárhelyi's model, denoted VA, that we simulate using its optimal set of parameters given in [4]. Tables III and IV list the results from 100 stochastic evaluations with the optimized set of parameters for each model. The average values of the mapped metrics (1 is best, 0 is worst) as well their relative variances are displayed. The last line corresponds to the average inter-agent distance in meters. To remain consistent, we use the same time of experiment $T = 600s$ and the same accuracy of the Euler method $DeltaT = 0.01s$. In addition, we consider a delay $t_d = 0.2s$ in the communications (ie. access delay to the radio medium, delay of data packet transmission and propagation delay) and reckon that agents exchange information at the GPS frequency $f_{GPS} = 5Hz$.

The first important observation we can draw here is that the VA model has much lower performances than the original results of [4] reported in Table II. This can be explained by the fact that the author relies on small arenas in his simulations, leading to an indirect effect of cohesion, the agents having no choice but to head back toward the center of the arena. In our considerations, and to avoid this advantageous behaviour, we set a large enough value ($1250m$) for our arena length. Also the distribution of the obstacles is not

TABLE III: FOREST

	Regular			**Degraded**		
	VA	VAT	VOS	VA	VAT	VOS
Vel	**0.975**	**0.946**	0.032	**0.975**	**0.955**	0.055
σ	0.010	0.03	0.052	0.008	0.023	0.063
Col	0.301	**1**	0.793	0.286	**0.961**	0.799
σ	0.429	0.099	0.382	0.429	0.172	0.380
Clust	0.637	**0.98**	**0.923**	0.508	**0.938**	0.868
σ	0.148	0.085	0.13	0.118	0.121	0.163
Wall	1	1	1	1	1	1
σ	0	0	0	0	0	0
Corr	0.133	**0.712**	0.54	0.128	**0.698**	0.531
σ	0.068	0.106	0.12	0.06	0.12	0.112
Pow	0.033	0.53	0.517	0	0.045	0.031
σ	0.049	0.11	0.074	0	0.079	0.066
Dist	132.3	37.9	49.9	132.5	42.11	54.37

TABLE IV: CITY

	Regular			**Degraded**		
	VA	VAT	VOS	VA	VAT	VOS
Vel	**0.999**	**1**	0.484	**0.999**	**1**	0.501
σ	1.1e-5	0	0.095	4.8e-5	0	0.101
Col	0.71	**0.999**	**0.918**	0.654	**1**	0.86
σ	0.442	0.09	0.264	0.47	0	0.33
Clust	0.671	**0.985**	**0.939**	0.54	**0.915**	**0.925**
σ	0.18	0.065	0.142	0.197	0.17	0.165
Wall	1	1	1	1	1	1
σ	0	0	0	0	0	0
Corr	0.605	**0,912**	0.886	0.73	**0.945**	0.894
σ	0.165	0.067	0.082	0.112	0.04	0.073
Pow	0.512	**0.797**	0.684	0.335	**0.777**	0.573
σ	0.205	0.092	0.073	0.286	0.16	0.204
Dist	82.19	29.4	44.3	86.76	33.8	45.55

explicitly mentioned in [4] which obviously impacts most of the metrics. Finally, taking into account a radio propagation model also adds a new constraint to the model that was not considered in the initial work. The drawbacks of not adding an attraction term are even more visible on the *forest* environment where the cluster parameter is relatively low, meaning there has been some fragmentation (Clust=0.637 in Table III). One may also wonder why adding an attraction term for the VAT model does not create more collisions. This can be explained by the fact that this attraction term is only effective above a precise inter-agent distance with a bounded resulting inertia preventing oscillations and hence collisions. The fact that the VAT model is also designed and optimized for **degraded** communications, and therefore applies the *neighbour filtering*, is one more reason to explain VA and VAT differences.

1) Maintaining the Connection: One of our goal in this article was to implement models capable of preventing the undesired effect of perpetual fragmentation. We can see in both tables that this objective is mostly satisfied. Indeed, for both VAT and VOS, the average *cluster* metric is high, $0.868 \leq$ Clust ≤ 0.985. This means that even if fragmentation occurred, the resulting clusters managed to repair broken connections and got back to a single cluster. Partial fragmentation was to be expected especially in the *forest*

environment as obstacles create frequent communication outages and interaction interruptions

2) Received Power and Collision: The inter-agent distance is a resulting parameter of all interactions and is mostly optimized by the *received power* metric but also the *collision* one. Agents must lie within a restricted range of distances between each other in order to be far enough to avoid collisions but close enough to remain connected. Please note that in these tables, a low value of the *received power* doesn't mean that the connection is lost. For instance in Table IV, we have Pow $= 0.573$ for the VOS model with *degraded* communications, but this is equivalent to a value of $P_R = -59.4dBm$, meaning that the communication was possible on average. As a comparison, in Table III, for VAT model with *degraded* communications, Pow $= 0.045 \simeq -71.7dBm$ ($-70dBm$ being the lowest acceptable value). This confirms the fact that, even if the communication is mostly broken, whenever they can, agents manage to get back to a nominal flocking behaviour.

3) Environment Overfitting: As mentioned earlier, the models we simulate are not optimised on the environments we use for the comparison. Therefore, there is a risk of overfitting a particular obstacle distribution. We can observe it for the VOS model in Table III where the average *velocity* metric is low, $0.032 \leq$ Vel ≤ 0.055, equivalent to 60% of the desired velocity v^{flock}. Although, in Table I, Vel$= 0.612$, the number of obstacle is around 5 times smaller. Within the *forest* environment, there are many obstacles close to each other leading to a "cage effect" and hindering the flock movements. It also creates many oscillations $0.531 \leq$ Corr ≤ 0.54 and potential collisions $0.793 \leq$ Col ≤ 0.799 (see video). The VOS model is hence not robust to the variation of obstacle distribution.

4) Regular/Degraded: The resulting effects of the *degraded* communication model can be observed in both tables. Moreover, the last line which concerns the inter-agent distance shows that this mode will increase the average distance between agents and even more when in the *forest* environment. However, the VAT model seems to be very resilient and robust to losses introduced by the *degraded* mode on its received power which makes it a valuable model.

VI. CONCLUSION

In this article, we proposed two flocking models based on the state of the art (VAT Vásárhelyi + Attraction and VOS Vásárhelyi + Olfati-Saber) to deal with degraded communications in presence of obstacles. We compared models via simulations integrating a Log Distance Path Loss model that takes into account the propagation inside the obstacles. With this evaluation environment, it was possible to analyse how flocks are affected or robust to degraded communications in complex environments. From the results, we can claim that the VAT model shows more encouraging performances than VOS and the original Vásárhelyi's model.

Even if the optimization has been conducted here on a single "generic" environment, it could be interesting to systematically optimize the models in each used environment. We then plan to design adaptive flocking strategies capable of optimally evolving in various environments with different types of communication. We also plan to carry out experiments with quadrirotor UAVs, in order to measure model efficiency in real environments.

REFERENCES

[1] Craig W. Reynolds. Flocks, herds and schools: A distributed behavioral model. *SIGGRAPH Comput. Graph.*, 21(4):25–34, 1987.

[2] Reza Olfati-Saber. Flocking for multi-agent dynamic systems: algorithms and theory. *IEEE Trans. Automat. Contr.*, 51(3):401–420, 2006.

[3] Heng Li, Jun Peng, Weirong Liu, Jing Wang, Jiangang Liu, and Zhiwu Huang. Flocking control for multi-agent systems with communication optimization. pages 2056–2061, 06 2013.

[4] G Vásárhelyi, C Virágh, G Somorjai, T Nepusz, AE Eiben, and T Vicsek. Optimized flocking of autonomous drones in confined environments. *Science Robotics*, 3(20), 2018.

[5] G. Wen, Z. Duan, H. Su, G. Chen, and W. Yu. A connectivity-preserving flocking algorithm for multi-agent dynamical systems with bounded potential function. *IET Control Theory Applications*, 6(6):813–821, 2012.

[6] B. Fraser, R. Hunjet, and C. Szabo. Simulating the effect of degraded wireless communications on emergent behavior. In *2017 Winter Simulation Conference (WSC)*, pages 4081–4092, 2017.

[7] Csaba Virágh, Gábor Vásárhelyi, Norbert Tarcai, Tamás Szörényi, Gergo Somorjai, Tamás Nepusz, and Tamás Vicsek. Flocking algorithm for autonomous flying robots. *Bioinspiration & Biomimetics*, 9(2):025012, may 2014.

[8] Noury Bouraqadi and Arnaud Doniec. Flocking-based multi-robot exploration. In *4th National Conference on "Control Architectures of Robots"*, Toulouse, France, 2009.

[9] G. W. Gamage, G. K. I. Mann, and R. G. Gosine. Leader follower based formation control strategies for nonholonomic mobile robots: Design, implementation and experimental validation. In *Proceedings of the 2010 American Control Conference*, pages 224–229, 2010.

[10] S. S. Ge and Cheng-Heng Fua. Queues and artificial potential trenches for multirobot formations. *IEEE Transactions on Robotics*, 21(4):646–656, 2005.

[11] T. Balch and R. C. Arkin. Behavior-based formation control for multirobot teams. *IEEE Transactions on Robotics and Automation*, 14(6):926–939, 1998.

[12] N. H. M. Li and H. H. T. Liu. Formation uav flight control using virtual structure and motion synchronization. In *2008 American Control Conference*, pages 1782–1787, 2008.

[13] Chao Wang, Jian Wang, Yuan Shen, and Xudong Zhang. Autonomous navigation of uavs in large-scale complex environments: A deep reinforcement learning approach. *Transactions on Vehicular Technology*, 68(3):2124–2136, 2018.

[14] Ronny Lim and W. Sheng. Hybrid system of reinforcement learning and flocking control in multi-robot domain. 2016.

[15] H. M. La and W. Sheng. Flocking control of a mobile sensor network to track and observe a moving target. In *2009 IEEE International Conference on Robotics and Automation*, pages 3129–3134, 2009.

[16] Guanghui Wen, Zhisheng Duan, Housheng Su, Guanrong Chen, and Wenwu Yu. A connectivity-preserving flocking algorithm for nonlinear multi-agent systems with bounded potential function. *Proceedings of the 30th Chinese Control Conference, CCC 2011*, 01 2011.

[17] Tamás Vicsek, András Czirok, Eshel Ben-Jacob, Inon Cohen, and Ofer Shochet. Novel type of phase transition in a system of self-driven particules. *Physical review letters*, 75(6):1226, 1995.

[18] Eric Frew Spencer Watza, Ramya Kanlapuli. Hybrid rf propagation model using itm and gaussian processes for communication-aware planning. In *RSS 2017 RCW Workshop*, 2017.

[19] Theodore Rappaport. *Wireless Communications: Principles and Practice*. Prentice Hall PTR, USA, 2nd edition, 2001.

[20] K. Deb and H. Jain. An evolutionary many-objective optimization algorithm using reference-point-based nondominated sorting approach, part i: Solving problems with box constraints. *IEEE Transactions on Evolutionary Computation*, 18(4):577–601, 2014.

[21] J. Blank and K. Deb. Pymoo: Multi-objective optimization in python. *IEEE Access*, 8:89497–89509, 2020.